Supporting Information

Development of a ^{99m}Tc-Labeled Single-Domain Antibody for SPECT/CT Assessment of HER2 Expression in Breast Cancer

Lingzhou Zhao,[†] Changcun Liu,[†] Yan Xing,[†] Jin He,[‡] Jim O'Doherty,[§] Wenhua Huang,[‖] and Jinhua Zhao[*,†]

[†]Department of Nuclear Medicine, Shanghai General Hospital, Shanghai Jiao Tong University School of Medicine, Shanghai 200080, China

[‡]Department of Pathology, Shanghai General Hospital, Shanghai Jiao Tong University School of Medicine, Shanghai 200080, China

[§]Siemens Healthineers, Malvern, Pennsylvania 19355, USA

[‖]Nanomab Technology Limited, Shanghai 200080, China

Correspondence to: Jinhua Zhao, Professor, Department of Nuclear Medicine, Shanghai General Hospital, Shanghai Jiao Tong University School of Medicine, No. 100 Haining Rd., Shanghai, 200080, China, Tel.: 86-21-37798352, E-mail: zhaojinhua1963@126.com

Reagents. Phosphate-buffered saline (PBS, pH = 7.4), PBS containing 0.1% Tween 20 (0.1% PBST), human HER2 antigen, 96-well ELISA plate, bovine serum albumin, horseradish peroxidase-conjugated anti-His tag detection antibody, tetramethyl benzidine dilution, and tricarbonyl kit were supplied by NanoMab (Shanghai, China). The tumor-bearing mice were purchased from Shanghai Model Organisms Center (Shanghai, China). All other chemicals and solvents were supplied by Sinopharm Chemical Reagent Co., Ltd. (Shanghai, China).

NM-02 production and formulation. The NM-02 was produced according to good-manufacturing-practice standards. In short, NM-02 was screened and selected from a phage display library generated from the peripheral blood lymphoctyes of *Camelus bactrianus* immunized against human HER2 extracellular domain protein. The sequence of NM-02 with a C-terminal hexahistidine tail was subcloned into the pE7 expression vector and produced in *Escherichia coli* BLR (DE3). Subsequently, the expressed NM-02 was purified from periplasmic extracts using anion exchange chromatography on Q Sepharose (GE Healthcare, USA) and was buffer-exchanged to PBS with gel filtration on Superdex 75 resin (GE Healthcare, USA). The Mustang Q XT5 membrane (Pall, USA) was used to remove endotoxins from the concentrated NM-02. Finally, the NM-02 products were aseptically dispensed into septum-sealed sterile glass vials at a concentration of 2.0 mg/mL in 100 μL PBS and stored at −80 ºC.

Binding assay. The binding affinity of NM-02 to HER2 was evaluated by enzyme-linked immunosorbnent assay (ELISA). Briefly, 2 μg/mL of human HER2 antigen in carbonate-bicarbonate buffer was coated on a 96-well ELISA plate at 4 ºC overnight.

Then the plate was washed 3 times with PBS and blocked in 1% bovine serum albumin in PBS at room temperature for 2 h. After washing the plate 3 times with PBS, 100 μL of NM-02 solution at different concentrations (0.1-100 nM) was added to the plate and incubated at 37ºC for 1 h. Subsequently, the plate was washed 4 times with 0.1% PBST and added the horseradish peroxidase-conjugated anti-His tag detection antibody. After incubation 1 h at 37 ºC, the plate was washed a further 4 times with 0.1% PBST and then developed by applying tetramethyl benzidine dilution for 10 min at room temperature. The reaction was stopped with H_2SO_4 (2 M) and the absorbance at 450 nm was determined using a microplate reader (SpectraMax i3x, Molecular Devices). As shown in Figure S3a, NM-02 can specifically bind to human HER2 with a dissociation constant (Kd) of 1.2 nM. Then the impact of ^{99m}Tc radiolabeling on the binding of NM-02 to HER2 was studied using the same ELISA assay. Figure S3b indicates that there is no significant difference between the NM-02 and the NM-02 after ^{99m}Tc radiolabeling in terms of binding affinity to HER2, suggesting good specificity of NM-02 *in vitro*.

Preparation of the $[^{99m}Tc(OH_2)_3(CO)_3]^+$ complex. All reagents used in radiolabeling, including preparation of the $[^{99m}Tc(OH_2)_3(CO)_3]^+$ complex and ^{99m}Tc-NM-02, were in accordance with GMP standards. The ^{99m}Tc-pertechnetate ($Na^{99m}TcO_4$) solution purchased from Shanghai GMS Pharmaceutical Co., Ltd (Shanghai, China), was obtained from a ^{99}Mo/^{99m}Tc generator. The $[^{99m}Tc(OH_2)_3(CO)_3]^+$ complex was manufactured using a tricarbonyl kit containing 4.5 mg $Na_2[H_3BCO_2]$, 2.85 mg $Na_2B_4O_7 \cdot 10H_2O$, 7.15 mg Na_2CO_3, and 8.5 mg $Na_2C_4H_4O_6 \cdot 2H_2O$ in a small glass vial

under argon. One milliliter of $Na^{99m}TcO^4$ solution (3330–5032 MBq) was added to the vial, and the vial was incubated in a boiling water bath for 30 minutes. Subsequently, the vial was removed from the water bath and cooled to room temperature. After adjusting its pH to 7.0-7.5 by addition of 180 μL HCl (1.0 M), the radiochemical purity (RCP) of the $[^{99m}Tc(OH_2)_3(CO)_3]^+$ complex was analyzed by instant thin-layer chromatography (ITLC) using silica gel 60 F254 TLC plates (Merck, Darmstadt, Germany) and ITLC-SG glass microfiber chromatography paper (Agilent, Folsom, CA, USA). The $[^{99m}Tc(OH_2)_3(CO)_3]^+$ complex showed a broad peak with an average retention factor (R_f) of 0.4-0.5 in the TLC plate using 1% HCl in methanol as the mobile phase, whereas $^{99m}TcO^{4-}$ had an R_f of 1 (Figure S4a). The R_f values of colloidal ^{99m}Tc and the $[^{99m}Tc(OH_2)_3(CO)_3]^+$ complex were 0 and 1, respectively, in the ITLC-SG paper using citrate buffer (pH 5.4) as the mobile phase (Figure S4b). The RCP was calculated as the ^{99m}Tc radioactivity associated with the $[^{99m}Tc(OH_2)_3(CO)_3]^+$ complex as a percentage of the total ^{99m}Tc radioactivity on the paper. Only $[^{99m}Tc(OH_2)_3(CO)_3]^+$ complex with a high RCP (>95%) was used for subsequent NM-02 radiolabeling.

Preparation and quality control of ^{99m}Tc-NM-02. For NM-02 radiolabeling, 400 μL of the formed $[^{99m}Tc(OH_2)_3(CO)_3]^+$ complex, corresponding to 977–1539 MBq, was immediately mixed with 200 μg of NM-02 in 100 μL PBS. The mixture was incubated at 50 °C in a water bath for 1 h to prepare the ^{99m}Tc-NM-02. Its RCP was assessed using ITLC, with an R_f of 0 in TLC-SG paper using a citrate buffer (pH 5.4) as the mobile phase (Figure S4c); the unreacted $[^{99m}Tc(OH_2)_3(CO)_3]^+$ complex and $^{99m}TcO^{4-}$ both had R_f values of 1 under the same conditions. The RCP was calculated as the ^{99m}Tc

radioactivity associated with ^{99m}Tc-NM-02 as a percentage of the total ^{99m}Tc radioactivity on the paper. Consequently, 1.5 mL saline was added to the vial to bring the total volume to 2.0 mL. Other quality control tests, including visual check and pH and endotoxin testing, were performed. Only ^{99m}Tc-NM-02 with an RCP >95%, pH = 7.0-7.5, and endotoxin levels of <15 EU/mL with a colorless, clear appearance was used in this study. For patient injection, 1.0 mL of the final solution was withdrawn aseptically into a 2.0-mL syringe, corresponding to 406–510 MBq ^{99m}Tc-NM-02 containing 100 μg NM-02. The *in vitro* stabilities were confirmed by measuring the RCPs of ^{99m}Tc-NM-02 in PBS at room temperature and in fetal bovine serum (FBS) at 37 °C within 6 h. No obvious changes were found in their radiochemical purities, suggesting excellent *in vitro* stability for potential clinical applications (Figure S4d).

Micro-SPECT/CT imaging. The imaging performance of ^{99m}Tc-NM-02 was validated *in vivo* using tumor-bearing mice and animal experiments were performed using the protocol approved by the ethical committee of Shanghai General Hospital. Briefly, 37 MBq ^{99m}Tc-NM-02 (corresponding to 10 μg of NM-02) was intravenously injected into the mice bearing HER2-positive subcutaneous BT474 tumors and HER2-negative subcutaneous MDA-MB-453 tumors, respectively. For comparison, the same dose of ^{99m}Tc-NM-02 was intravenously injected into the mice bearing HER2-positive subcutaneous BT474 tumors that were treated with 2 mg of Trastuzuamb or Pertuzuamb four days before imaging, and 37 MBq ^{99m}Tc-NM-02 and 200 μg of NM-02 were also co-injected into the HER2 positive tumor-bearing mice for the blocking experiment. Micro-SPECT/CT images were acquired at 1.5 h after injection using U-SPECT/CT

scanner (Milabs, Utrecht, the Netherlands). As shown in Figure S5, the ^{99m}Tc-NM-02 can be mainly found in the kidneys and bladder, with a low level of radioactivity in background and a mild uptake in the liver, spleen and intestines, indicating its favorable biodistribution. Meanwhile, obvious ^{99m}Tc-NM-02 accumulation can be observed in the HER2-positive tumors (BT474) with or without the presence of Trastuzuamb or Pertuzuamb, demonstrating the specific tumor uptake and no competition with Trastuzumab and Pertuzumab for HER2 Imaging. On the contrary, no obvious tracer uptake displays in the HER2-positive tumors blocked by NM-02 and HER2-negative tumors (MDA-MB-453). These results suggest that ^{99m}Tc-NM-02 has good specificity *in vivo* and can be the potential candidate for SPECT/CT imaging of HER2 expression in patients with breast cancer.

Patient selection. Adult women who met the inclusion criteria were invited to participate in this study. The inclusion criteria were as follows: those with pathologically confirmed breast cancer; who agreed to participate in this study and signed the informed consent form; who had AST, ALT, BUN, and Cr levels of no more than twice the normal value; and had no currently active infectious diseases, such as hepatitis A infection, hepatitis B infection, HIV infection, and tuberculosis. The exclusion criteria were as follows: those who were male; pregnant or breastfeeding; had uncertain or untested human epidermal growth factor receptor 2 (HER2) expression levels; pacemakers; known abnormal liver, kidney, or thyroid function; serious active infection; recent myocardial infarction or other cardiogenic events requiring hospitalization; and were unlikely to cooperate with the requirements of this clinical

study after evaluation by the investigator. Patients with severe allergic reactions, persistent allergic reactions, willingness to quit the clinical study, and unlikelihood of continuing this clinical study after evaluation by the investigator were also excluded.

SPECT/CT acquisition protocol and quantitative analysis. The speed of bed motion for the whole-body SPECT imaging was set at 10 cm/min, with a total scan time of about 20 minutes. Local SPECT/CT was performed over 360° in 60 steps per full rotation, with a 20-s acquisition per step. Low-dose CT was used for attenuation correction and localization during tomographic acquisitions, with scan parameters as follows: 120 kV, 180 mA, 512 × 512 matrix, 3.75-mm thickness, and a large field of view. All SPECT scans were performed using low-energy high-resolution collimators in a 20% energy window centered around 140 keV with a 256 × 1024 matrix for whole-body SPECT imaging and a 128 × 128 matrix for local SPECT imaging. SPECT/CT images were reconstructed using the Xeleris Functional Imaging Workstation (GE Healthcare).

The Q.Metrix software package was used to perform quantitative measurements of the SPECT data. The acquisition information was input into the software, including the patient height and weight, tracer activities in the full and empty syringes, administration time, scan time, and camera sensitivity. The volumes of interest were chosen using thresholding methods, with an NM threshold of 0.4 on SPECT images. The maximum standardized uptake value was automatically calculated in the system.

Radiation dosimetry calculations. For radiation dosimetry calculations, three patients underwent whole-body SPECT imaging at five time points, including 10 min,

1 h, 2 h, 3 h, and 24 h after injection, with a calibration source of 37 MBq above the head of each patient. The OLINDA/EXM dose calculation software 1.1 was used to calculate dosimetry according to the protocol reported in our previous study.

Safety assessment. For safety assessment, all patients underwent vital sign evaluation and clinical laboratory testing. Vital signs, including the blood pressure, heart rate, respiration rate, and body temperature, were recorded during the screening period, before injection, and then every 1 h up to 4 h after injection and the first 48 h after the SPECT/CT scan. Clinical laboratory testing was performed before and 48 h after injection. The testing included standard hematologic and comprehensive metabolic panels, including the evaluation of red blood cells, hemoglobin, white blood cells, neutrophils, lymphocytes, platelets, creatinine, monocytes, eosinophils, basophils, blood urea nitrogen, calcium, sodium, potassium, lactate dehydrogenase, alanine transaminase, aspartate aminotransferase, alkaline phosphatase, total serum bilirubin, and serum albumin. Additional phone interviews were performed 1 week after the SPECT/CT scan for patients to record their subjective adverse experiences.

Statistics. Data are reported as mean ± standard deviation and were analyzed using SPSS software (Version 24.0). A one-way analysis of variance was performed to evaluate the significance of the data. A P-value of less than 0.05 was considered statistically significant.

Table S1. Patient characteristics

Patient no.	Age (y)	IA (MBq)	Tumor type	ER/PR	HER2 IHC	HER2 FISH		Tumor size (cm)	Primary tumor position	Metastatic lesion	Clinical staging
						Positivity	Ratio				
BR001	53	509.9	IPC	-/-	3+	A	A	2.9×5.4×4.7	right	right axillary lymph node	T3N1M0
BR002	47	499.9	IDC	-/-	0	-	0.88	1.8×1.3×1.6	bilateral	left axillary lymph nodes	T1cN1M0
BR003	41	409.6	IDC	+/+	0	-	1.06	3.5×6.1×2.7	bilateral	bilateral axillary lymph nodes	T3cN2aM0
BR004	51	472.1	IDC	+/-	0	-	0.88	2.0×1.8×2.0	left	NA	T2N0M0
BR005	66	405.5	IDC	-/-	0	-	1.27	4.0×3.0×2.0	left	NA	T1N0M0
BR006	50	485.4	IDC	+/-	3+	A	A	7.0×3.0×3.5	right	right axillary lymph nodes and right supraclavicular nodes	T4bcN3cM0
BR007	62	465.8	ILC	+/+	0	-	1.08	1.0×0.5×0.5	left	NA	T1bN0M0
BR008	57	421.8	IDC	+/+	2+	-	1.53	2.5×1.5×1.3	left	left axillary lymph node	T2N1M0
BR009	54	465.8	IDC	+/+	2+	-	1.05	3.1×2.0×3.3	right	right axillary lymph node	T2N1M0
BR010	41	446.2	IDC	+/+	3+	+	1.17	8.1×2.0×5.5	right	right axillary lymph nodes	T3cN2aM0

IA = injected activity; ER = estrogen receptor; PR = progesterone receptor; IPC = invasive papillary carcinoma; IDC = invasive ductal carcinoma; ILC = invasive lobular carcinoma; A = absent. Clinical staging was determined using the eighth edition of the American Joint Committee on Cancer staging for breast cancer.

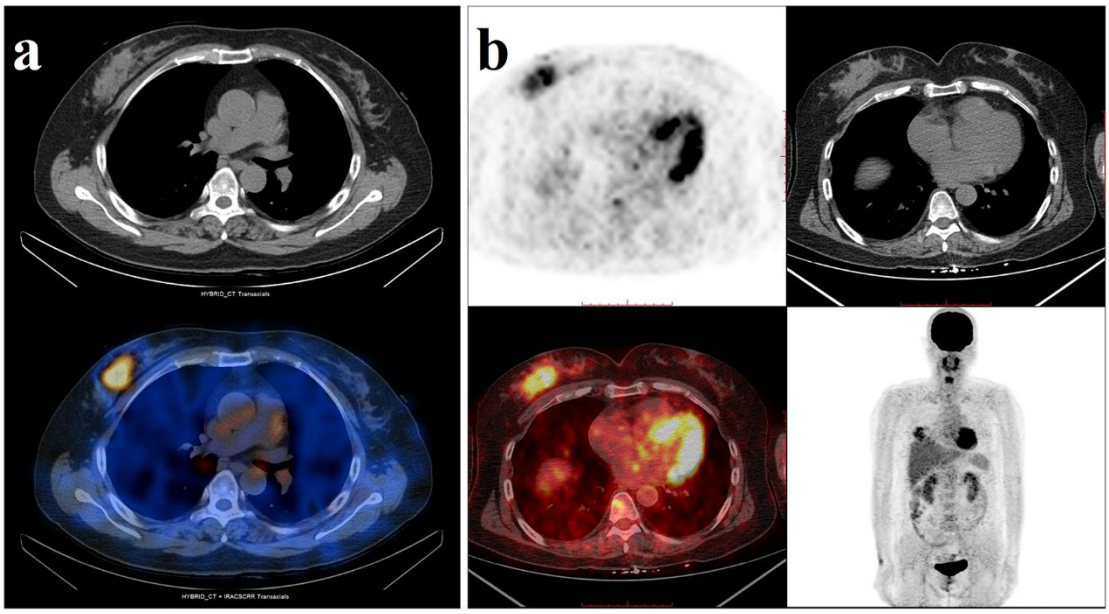

Figure S1. Images of Patient BR001 at 1 h after injection of ^{99m}Tc-NM-02 (a) and ^{18}F-FDG (b), respectively.

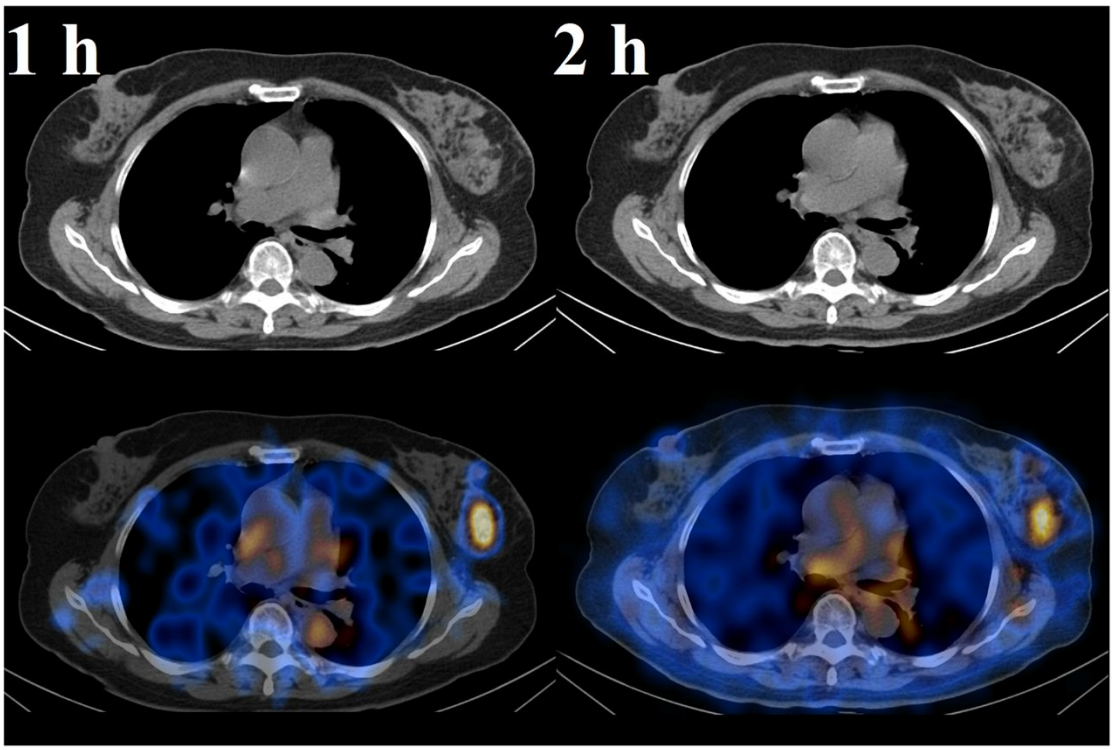

Figure S2. SPECT/CT images of Patient BR005 at 1 and 2 h after injection.

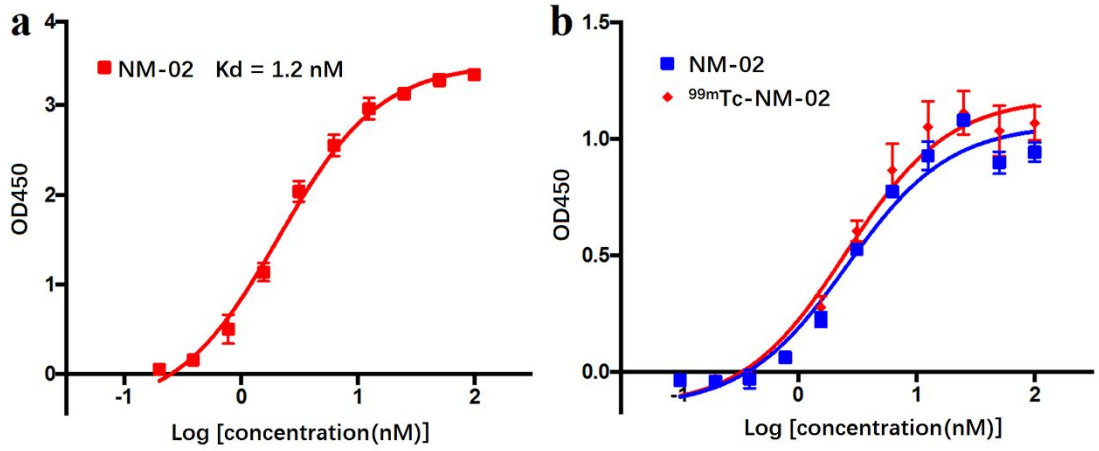

Figure S3. (a) ELISA analysis of the binding affinity of NM-02 to HER2. (b) ELISA analysis of the binding affinity of NM-02 before and after ^{99m}Tc radiolabeling. The synthesized ^{99m}Tc-NM-02 was stored at 4 °C for at least 3 days until no detectable gamma emission before ELISA assay.

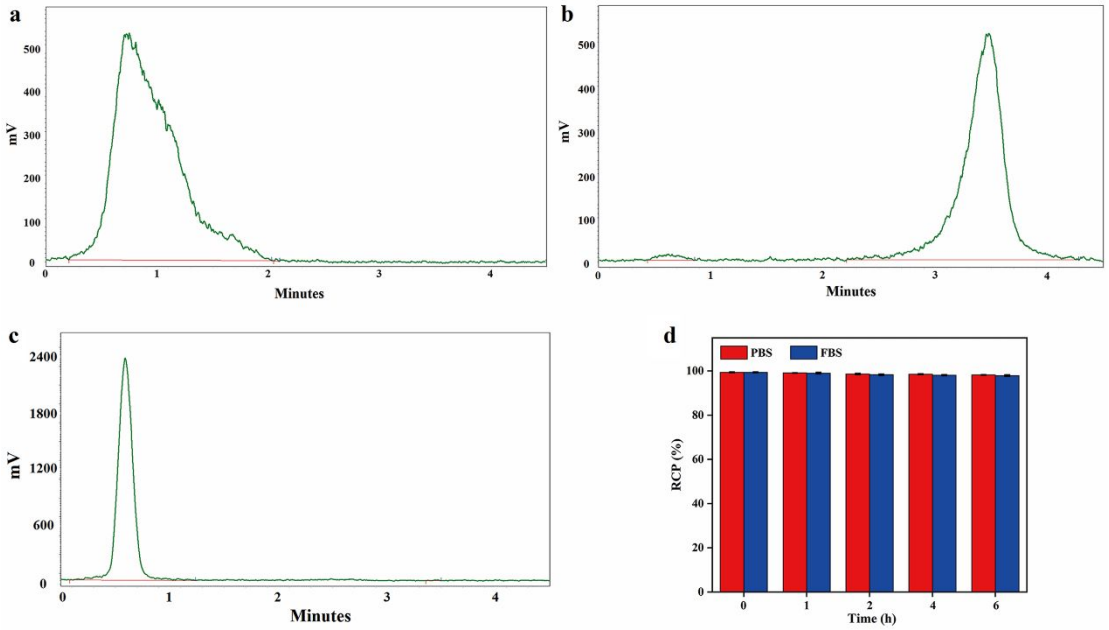

Figure S4. ITLC results of $[^{99m}Tc(OH_2)_3(CO)_3]^+$ complex using the methanol containing 1% HCl (a) and the citrate buffer (b) as the mobile phases, respectively. The ITLC results of ^{99m}Tc-NM-02 using the citrate buffer as the mobile phase (c), and the RCPs of ^{99m}Tc-NM-02 in PBS at room temperature or FBS at 37 °C for 0, 1, 2, 4 and 6 h, respectively (d).

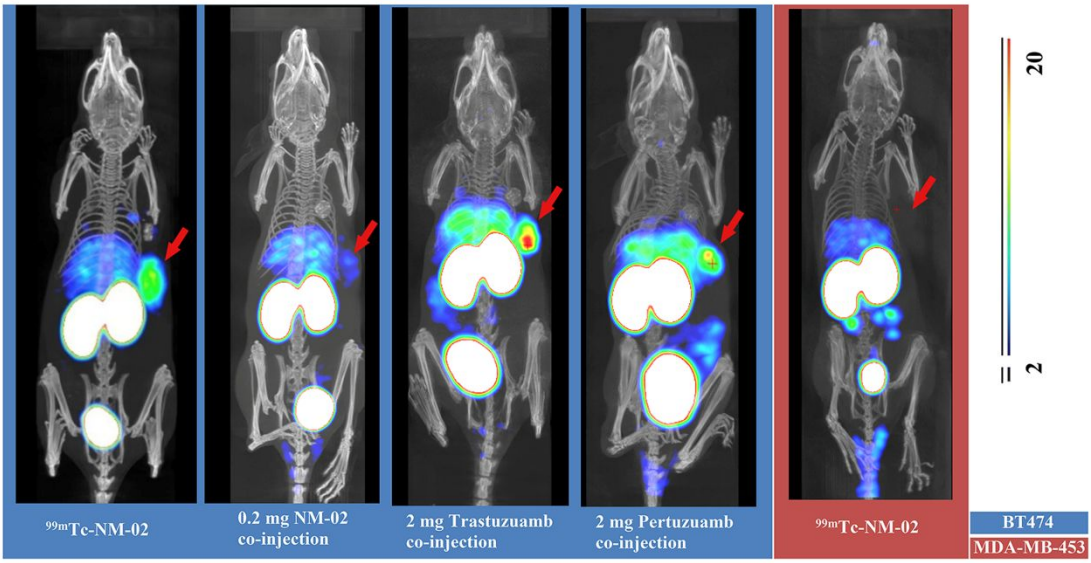

Figure S5. Micro-SPECT/CT images of ^{99m}Tc-NM-02 in the mice bearing HER2-positive subcutaneous BT474 tumors and HER2-negative subcutaneous MDA-MB-453 tumors at 1.5 h after injection. Red arrow indicates tumor.